International Journal of Engineering and Applied Physics (IJEAP)
Vol. 4, No. 3, September 2024, pp. 1055~1067
ISSN: 2737-8071

Radionuclides Distribution in Al-Qayyarah Oil Wells and refinery in Nineveh Government, Iraq

Zainab Mowafaq Maria[1], Laith Ahmed Najam[2], Taha Yaseen Wais[3,4], Berivan F. Namq[5]
[1,2,3]Department of Physics , College of Science, University of Mosul, Mosul, Iraq
[4]Chemical, Biological and Radiological Safety and Security Division, University of Mosul, Mosul, Iraq
[5]Department of Basic Science, College of Dentistry, University of Kirkuk, Kirkuk, Iraq

Article Info

Article history:

Received Jan 23, 2024
Revised July 13, 2024
Accepted Aug 14, 2024

Keywords:

Specific Activity
gamma spectroscopy
Oil wells
Radionuclides
Nineveh Government

ABSTRACT

This work presents a study of radioactivity in soil samples collected from oil well sites of the Al-Qayyarah Oil Wells and refinery in Nineveh Government, Iraq. The study utilized spectroscopy system with NaI(Tl). The average activity concentrations observed were 30.58±0.38 Bq/kg for ^{226}Ra, 19.98±0.57 Bq/kg for ^{232}Th, 292.32 ±10.28 Bq/kg for ^{40}K. These results were compared to the average worldwide values, and it was found that the values for some sites exceeded the allowable worldwide levels. Additionally, various hazard indices were calculated. The radium equivalent activity (Ra_{eq}) was 81.97 Bq/kg, the absorbed gamma dose rate (D_R) was 38.55 nGy/h, the annual effective dose rate (AEDE) was 47.28 µSv/y outdoor and 189.13 µSv/y indoor, the external hazard (H_{ex}) was 0.22, the internal hazard (H_{in}) was 0.30, the gamma radiation representative level index (I_γ) was 0.60, the annual gonadal dose equivalent (AGDE) was 271.05, and the excess lifetime cancer risk was 165.48. Statistical analyses, including mean, median, standard deviation, kurtosis, skewness, box plots, frequency distributions, Quantile-quantile (Q-Q) plots, Pearson's correlation coefficient, principal component analysis (PCA), and cluster analysis, were conducted to further examine and explain the results.

This is an open access article under the CC BY license.

Corresponding Author:

Laith Ahmed Najam,
Department of Physics,
College of Science,
University of Mosul, Mosul, Iraq.
Email: prof.lai2014@gmail.com

1. INTRODUCTION

Radioactivity is a perpetual phenomenon that causes pollution of soil, water, air, and animal and plant food as a result of the presence of radionuclides produced by this phenomenon [1]. Iraq is considered one of the largest oil deposits in the world. In addition, this country faces a serious human-caused threat through environmental pollution from oil spills and gas flaring. Many oil companies are seeking for oil exploration and refining operations in this country, and the amount of radioactivity in the soil varies over a wide range and is one of the sources of continuous exposure of humans to terrestrial radioactivity. Exposure to terrestrial radioactivity from soil depends on many factors such as soil types . Soil is one of the most important elements of the environment that supplies humans with food, as it is the fragile layer that covers the rocks of the earth's crust and its thickness ranges from several centimeters to many meters, and

because it is a dynamic medium when it is polluted ,it leads to the pollution of air, food alike and water. Thus ,it becomes a long-term source of pollution [2, 3] .

According to geological explorations, the presence of radionuclides is from uranium, radium, thorium, since the early 1930's, when they were used as a means of exploration and search for oil samples, as the production of wastes such as metal deposits inside pipes, equipment or contaminated components during exploration [4].

Natural radioactive materials are present in different proportions in the outer put of the earth′s surface, which can be concentrated and increased during oil and gas production processes .The radioactive materials extracted during various industrial processes are known as TENORM, i.e. the technology that enhances naturally radioactive materials, TENORM are present in sludge, dredging products. Oil samples contain elevated levels of radiation to which workers may be exposed while working on equipment containing such materials, Uranium and thorium are present in the ground near oil and gas reservoirs, and during oil and gas extraction processes, the decay products of these nuclides come out with the water resulting from those processes, as a result of the dissolution of radium-226 and radium-228 in water, while uranium and thorium do not dissolve in water, and thus these radioactive materials are transmitted to the surface of the earth, which leads to radioactive effects and dangers for workers in oil fields and refineries, and the general public close to that areas and the environmen [5].

The present work aims to determine the specific activities of ^{226}Ra, ^{232}Th, and ^{40}K in soil samples collected from oil well sites of the Al-Qayyarah Oil Wells and refinery in Nineveh Governorate, Iraq. Additionally, the study evaluates the radium equivalent activity (Ra_{eq}), the absorbed dose (D_R), the annual effective dose rate (AEDE), the annual gonadal dose equivalent (AGDE) the Gamma radiation representative Index (I_γ), the external hazard index (H_{ex}), the internal hazard index (Hin), and the excess lifetime cancer risk (ELCR). The parameters gathered in this study could be added to a database of natural radioactivity levels, and the findings will provide information on the activity distribution of natural radionuclides and the radiation doses received by people who come into contact with this environment.

2. RESEARCH METHOD

2.1 Location of study

The district of Qayyarah is located in Nineveh Governorate in northern Iraq. The Qayyarah district is distinguished by its important geographical location, as it is situated on the main road connecting the cities of Mosul and Erbil. The center of the Qayyarah district is located approximately 35 kilometers northeast of the city of Mosul, as shown in Figure 1.Economically, the Qayyarah district primarily depends on agriculture and grazing. The residents of the area cultivate various agricultural crops such as wheat, barley, and vegetables. The residents also raise sheep and goats. In addition, the Qayyarah district contains many important archaeological and heritage sites, such as the ruins of the ancient Qayyarah Castle. The study targeted the Qayyarah oil fields, which are considered one of the most important oil fields in Nineveh Governorate, as they produce large quantities of crude oil. These oil fields are located approximately 35 kilometers northeast of the city of Mosul. The discovery and exploitation of these oil fields dates back to the 1970s, when national and foreign oil companies conducted extensive exploration and drilling operations in the area.

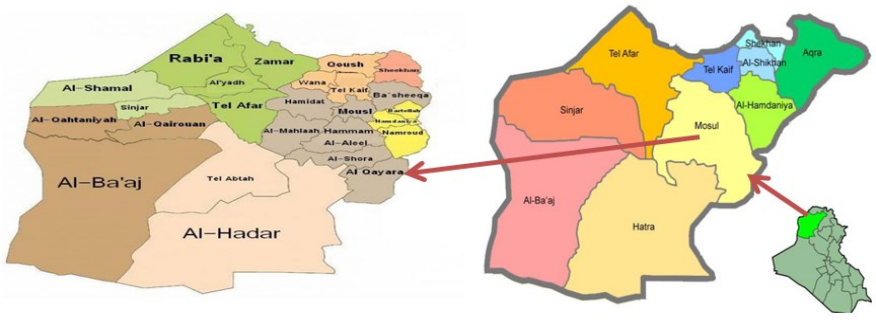

Figure 1: A map of Iraq showing the Al-Qayyarah district**.**

2.2 Sampling collection

Twenty-one samples were taken from the soils near oil fields and refinery in the district of Al-Qayyarah in Nineveh Governorate, where the sampling mechanism was according to approved global contexts, by specifying an area (1 m^2×1m^2) and a depth of (10-15 cm), in order to ensure the removal of

gravel and plankton and access to the surface soils. The mass of each sample was about 1 kg, then it was placed in plastic bags, Table 1 and Figure 2, show the coordinates of locations of the samples under study that were taken by the global positioning system [6-8] .

Figure 2: Sample collection points from Al-Qayyarah oil wells and refinery.

2.3 Preparation Techniques

After completing the process of collecting samples, the samples were dried using a thermal oven of the type (Luxel, Germany) operating in a temperature range (0-240ºC), where a temperature of 100ºC was used in this research for a period of one hour to get rid of moisture and ensure that the samples are dried well . Then, the samples were ground using an electric mill (Restch KG,Turkey) and sieved through a sieve with a diameter of 1 mm to obtain homogeneous samples. By means of a sensitive balance (KERRN ABS, Germany), 0.5 kg of soil samples under study were weighed to be placed in a Marneli container and kept for a month before conducting the analysis process in order to ensure the radioactive equilibrium between radium and its daughters [8].

2.4 Sampling and sample preparation

Gamma-ray spectrometry was used to estimate the activity concentrations of natural radionuclides in soil samples. The scintillation crystal of thallium-activated sodium iodide NaI(Tl) is coupled to photomultiplier tubes in this spectrometer apparatus. To minimize the influence of background radiation on the measurements, the detector is placed in the lead block when designing the geometry of the measuring system. Before counting the samples, the detector's efficiency and energy were calibrated for different energies of interest in the selected sample geometry, as described by the International Atomic Energy Agency's calibration protocols IAEA. The energy of the detector was calibrated using standard sources supplied by IAEA, where the standard sources (^{60}Co, ^{137}Cs, ^{241}Am, ^{22}Na and ^{133}Ba) were placed on the detector holder at a distance of 5 cm from the detector for a period of 90 seconds, as shown in Figure 3. after which the efficiency calibration process of the detector was carried out. Using a standard source also supplied by IAEA, ^{152}Eu was used, as shown in Figure 4. The intensity of the 295.2 keV and 609.3 keV gamma lines of ^{214}Pb and ^{214}Bi, respectively, was used to measure the ^{226}Ra activity of the samples. The gamma lines 911.21 keV and 338.32 keV of ^{228}Ac were used to generate ^{232}Th activity with intensities of 26.6% and 11.27%, respectively. The gamma ray line 1460.70 keV was used to obtain ^{40}K. The specific activity was calculated by placing the sample in front of the detector and recording the gamma-ray spectrum for (18,000 seconds) and the program (UCS-20) in the computer draws the spectrum, where the activity concentration for each sample is calculated by the following equation (1) [9-11]:

$$\mathrm{A}\ (Bq/kg) = \frac{(\mathrm{N} - \mathrm{B})}{\varepsilon \times \mathrm{I} \times \mathrm{t} \times \mathrm{m}} \quad (1)$$

Where, N-B is the net peak count rate (count/sec), (ε) is the efficiency of detecting gamma rays, I is the probability of gamma emission, t is the time of the spectrum analysis and m is the weight of the soil samples. The minimum detectable activity was calculated from the peak areas of the background spectrum (B) at a 95% confidence level using Equation (2) [12]:

$$\text{MDA} = \frac{1.64 \times \sqrt{B}}{\varepsilon \times I \times t \times m} \quad (2)$$

The minimum detectable activities for ^{226}Ra, ^{232}Th, and ^{40}K in the samples were determined to be 1.95 Bq/kg, 1.47 Bq/kg, and 8.15 Bq/kg, respectively.

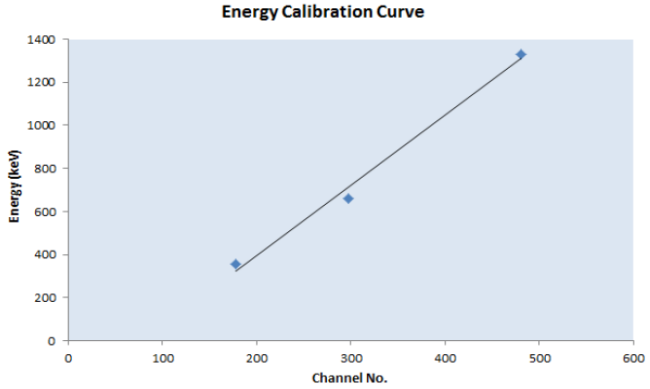

Figure 3. The energy calibration curve for the NaI(Tl) detector.

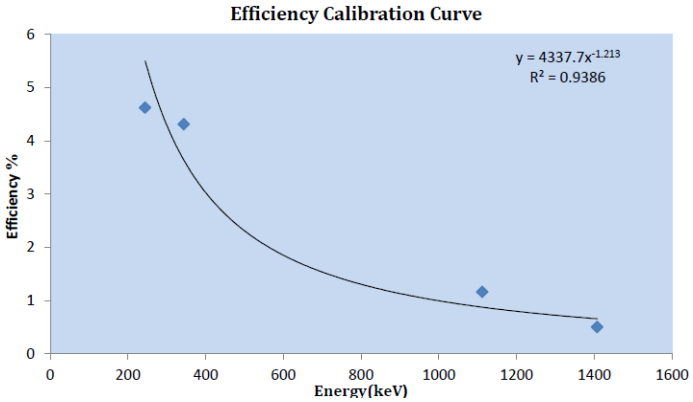

Figure 4. The calibration curve depicting the efficiency of the NaI(Tl) detector

2.5 Radiological parameter calculation

As radiation comes from naturally occurring radionuclides residing in close proximity to the terrestrial areas of the sampling locations, care should be made to limit exposure to persons handling soil samples. As a result, radiation indices can be used to evaluate the gamma-ray radiation dangers caused by the listed radionuclides.

2.5.1 Radium equivalent activity (Ra_{eq})

The presence of ^{226}Ra, ^{232}Th, and ^{40}K in raw soil samples is typically used to estimate their normal radioactivity. Minerals from soil samples are also utilized, as well as soils and light sands that have been abandoned by businesses and building firms. The idea of radium equivalent makes it possible to represent the gamma output of various combinations of radium, thorium, and ^{40}K in soil samples from various sites using just one index or number. Due to radon and its daughters, Raeq is related to both the internal and external gamma doses. This formula is used to calculate it [13].

$$\text{Ra}_{\text{eq}}(\text{Bq/kg}) = \text{A}_{\text{Ra}} + 1.43\text{A}_{\text{Th}} + 0.077\text{A}_{\text{K}} \quad (3)$$

Where A_{Ra}, A_{Th} and A_K are the specific activities of ^{226}Ra, ^{232}Th and ^{40}K in (Bq/kg) respectively. For radiation exposure safety, the recommended upper limit of Ra_{eq} is 370 Bq/kg [14].

2.5.2 Absorbed gamma dose rate (D_R)

The radiation dose from radionuclides in soil is called the air absorbed dose rate. The absorbed dose rate directly affects the biological, radiological, and clinical impacts. The absorbed dose rate can be used to calculate risks to people handling samples near oil fields and the radiation threats from natural gamma rays on the Earth's surface. The provided equation was used to compute the external gamma dose absorption rate in air (nGy/h) at 1m above ground, based on the measured activity of ^{226}Ra, ^{232}Th, and

^{40}K in soil samples [13-15] .

$$D_R(nGy/h) = 0.462A_{Ra} + 0.604A_{Th} + 0.0417A_K \quad (4)$$

The conversion of ^{226}Ra, ^{232}Th, and ^{40}K are 0.462, 0.604, and 0.417 respectively.

2.5.3 Annual effective dose equivalent (AEDE)

The annual effective dose corresponding to the absorbed dose was calculated in order to evaluate the radiological risk to human health. The conversion factor from the dose absorbed in air to the effective dose and the external occupancy factor must be considered when estimating annual effective doses. According to the UNSCEAR (2000) reports, the outside occupation factor is (0.2), which indicates that individuals spend 20% of their time outside on average around the scientist, and the conversion factor (0.7 Sv/Gy) were both used to calculate the effective dose received by adults. The risk of radiation to human health can be calculated using the equation below [6, 14].

$$AEDE\ (mSv/y) = D_R(nGy/h) \times 8760h \times 0.2 \times 0.7SvGy^{-1} \times 10^{-6} \quad (5)$$

$$AEDE(mSv/y) = D_R \times 0.00123 \quad (6)$$

2.5.4 Gamma representative level index (I_γ)

The Gamma Representative level index (I_γ) was used to evaluate the gamma radiation dangerous levels related to the naturally occurring radionuclides in the oil samples. The representative level index of the oil samples can be used to calculate the potential risk from gamma radiation posed by the oil samples natural gamma emitters. The equation below is used to calculate it [14].

$$I_\gamma = \frac{1}{150A_{Ra}} + \frac{1}{100A_{Th}} + \frac{1}{1500A_K} \quad (7)$$

The safety value of this index is set at ≤ 1 [14].

2.5.5 Annual gonadal dose equivalent (AGDE)

It gauges the genetic significance of the annual dosage equivalent that the population's reproductive systems receive (gonads). In the same context, UNSCEAR considers the active bone marrow and bone surface cells to be the organs of interest (1988). As a result, the method below was used to compute the annual gonadal dose equivalent (AGDE) brought on by the particular activity of ^{226}Ra, ^{232}Th, and ^{40}K [15].

$$AGDE(\mu Sv/y) = 3.09A_{Ra} + 4.18A_{Th} + 0.314A_K \quad (8)$$

2.5.6 Internal Hazard Index (H_{in})

Thoron (^{220}Rn, the daughter product of ^{224}Ra) and radon (^{222}Rn, the daughter product of ^{226}Ra), two short-lived radionuclides, both release alpha particles that are harmful to the pulmonary system when inhaled. The internal hazard index helps to quantify this risk (H_{in}) [17].

$$H_{in} = \frac{A_{Ra}}{185Bq/kg} + \frac{A_{Th}}{259Bq/kg} + \frac{A_K}{4810Bq/kg} \quad (9)$$

For this index, the safety value is ≤ 1 [14].

2.5.7 External hazard index (H_{ex})

Another factor used to evaluate a material's radiological compatibility is its external hazard index. In other words, the radiation dosage anticipated to be supplied externally if a building is constructed using these materials is estimated using the measured activities in building materials. The model for calculating the external hazard index Hex is based on infinitely thick walls without windows and doors to serve as a criterion for limiting the radiation dose to this value. Equation (10) can be used to evaluate this index [10, 11].

$$H_{ex} = \frac{A_{Ra}}{370Bq/kg} + \frac{A_{Th}}{259Bq/kg} + \frac{A_K}{4810Bq/kg} \quad (10)$$

For this index, the safety value is ≤ 1[14].

3. RESULTS AND DISCUSSIONS

3.1 Specific activity of ^{226}Ra, ^{232}Th, and ^{40}K in soil

The radionuclides present in oil fields play a significant role in the overall radiation levels. Examples of these radionuclides include ^{226}Ra, ^{232}Th, and ^{40}K. These radionuclides can lead to exposure for workers in the oil fields as well as the nearby population. Accurately measuring this radiation is important. The extent of human exposure can be assessed by comparing the measured values to the recommended world standards. Table 1 presents the specific activity measurements of these radionuclides in samples taken from the areas surrounding the Qayyarah oil wells and refinery. The specific activity values for ^{226}Ra ranged from 14.24±0.66 to 53.73±1.29 Bq/kg, with an average of 30.58 ± 0.387 Bq/kg. For ^{232}Th, the values ranged from 12.61±0.92 to 32.53±1.41 Bq/kg, with an average of 19.98±0.57 Bq/kg. The ^{40}K values varied from 131.90±7.12 to 597.69±15.15 Bq/kg, with an average of 292.32 ± 10.289 Bq/kg. These average specific activity values for the radionuclides were within the worldwide average recommended by the UNSCEAR, which are 35 Bq/kg for ^{226}Ra, 30 Bq/kg for ^{232}Th, and 400 Bq/kg for ^{40}K [14]. Given the homogeneous geological composition of the study area, the variations in radioactivity levels between different sites are likely due to the enrichment process that has altered the composition of these radionuclides in the soil. This explains the higher specific activity of ^{226}Ra observed in certain locations, such as Qa3, Qa4, Qa11, Qa12, Qa16, Qa19, and Qa21. The ^{232}Th isotope values were within the permissible range across all sites, while the potassium ^{40}K isotope showed a significant increase in a few locations, but remained within the normal range recorded in Iraq. In general, the average specific activities of ^{226}Ra, ^{232}Th, and ^{40}K in the soil samples of the study area follow the order of ^{40}K > ^{226}Ra > ^{232}Th, as shown in Table 1.

Table 1. Coordinates of samples, and specific activity of ^{226}Ra, ^{232}Th, and ^{40}K in soil samples from the area near oil wells and refineries for the Al-Qayyarah.

Sample no.	Sample code	GPS Positions		Specific activity (Bq/kg)		
		Latitude	Longitude	^{226}Ra	^{232}Th	^{40}K
1	Qa1	34°35′78″N	39°63′480″E	26.33±0.85	21.75±1.13	214.23±9.07
2	Qa2	34°49′88″N	39°64′290″E	27.86±0.86	12.61±0.92	390.76±12.25
3	Qa3	34°42′90″N	39°63′292″E	34.16±0.41	30.317±1.33	393.84±12.30
4	Qa4	33°71′88″N	39°68′984″E	39.50±0.73	24.12±0.86	231.92±9.44
5	Qa5	34°28′92″N	39°64′391″E	20.58±0.71	19.13±1.14	165.38±5.23
6	Qa6	34°27′52″N	39°63′532″E	15.26±0.64	13.24±0.80	251.15±9.82
7	Qa7	34°42′21″N	39°65′104″E	22.89±0.84	19.99±0.96	231.92±9.44
8	Qa8	34°35′21″N	39°62′836″E	14.24±0.66	13.19±0.92	270.38±10.19
9	Qa9	34°17′83″N	39°64′513″E	20.15±0.79	15.42±1.02	293.46±10.62
10	Qa10	34°39′2″N	39°63′624″E	19.89±0.78	13.42±0.95	184.61±8.41
11	Qa11	34°38′85″N	39°64′691″E	46.65±1.17	18.56±1.10	378.46±12.06
12	Qa12	33°88′79″N	39°69′205″E	34.99±1.04	32.53±1.41	135.76±7.22
13	Qa13	34°98′87″N	39°66′923″E	32.29±1.00	20.36±1.10	186.53±8.47
14	Qa14	33°74′62″N	39°70′473″E	27.35±0.92	14.51±0.97	301.26±12.11
15	Qa15	34°23′8″N	39°65′682″E	34.36±0.99	16.05±1.03	389.61±12.24
16	Qa16	35°47′30″N	43°16′474″E	53.73±1.29	25.48±1.27	597.30±15.16
17	Qa17	35°47′20″N	43°16′536″E	31.75±0.99	25.93±1.51	131.92±7.12
18	Qa18	35°47′27″N	43°16′584″E	26.43±0.90	15.70±1.03	597.69±15.15
19	Qa19	35°47′8″N	43°16′528″E	39.65±0.69	24.61±1.22	135.76±7.29
20	Qa20	35°47′19″N	43°16′489″E	32.75±0.73	16.34±1.01	366.53±11.87
21	Qa21	35°47′21″N	43°16′355″E	41.34±1.19	26.47±1.34	290.38±10.56
Max				53.73±1.29	32.53±1.41	597.69±15.15
Min				14.24±0.66	12.61±0.92	131.90±7.12
Average				30.58±0.38	19.98±0.57	292.32 ±10.28
Worldwide Average				35	30	400

As indicated in Table 2, the specific activity values obtained from this study were compared with our measured specific activity of soil samples in some studies. The table shows that the specific activities of these radionuclides in the soil samples from Al-Qayyarah are within the range of values reported in the literature for other countries, such as Turkey, India, Nigeria, Pakistan, Iran, Saudi Arabia, Bangladesh, and different regions of Iraq (Mosul, Erbil, and Basra), with only minor differences where they may be slightly lower, higher, or comparable.Variations in radionuclide distribution may be the cause of the observed disparities. Along with other contributing elements, this is probably connected to the amount of radioactive minerals present as well as the geological, geochemical, and geographic origins of the raw materials employed [14]. Overall, the table provides a useful comparative analysis of the natural radioactivity of the soil in the study area with similar data from other parts of the world.

Table 2. Comparison of specific activity of ^{226}Ra, ^{232}Th, and ^{40}K in soil sample near oil wells in Al-Qayyarah with the results of various studies from different countries.

Country	Specific activity (Bq/kg)			References
	^{226}Ra	^{232}Th	^{40}K	
Turkey	24.5	51.8	344.9	[19]
Iraq, Mosul	11.05	23.93	226.6	[8]
Iraq, Erbil	25.61	20.15	326.64	[20]
India	47.0	106	--	[21]
Nigeria	41	29.7	412.5	[22]
Nigeria	75.6	21.3	128.6	[23]
Pakistan	45	67	878	[24]
Iran	31.5	23.5	615	[25]
Pakistan	45.31	58.39	244.99	[26]
Saudi Arabia	23.19	7.73	278	[27]
Bangladesh	21.76	36.64	477.57	[28]
Iraq, Basra	33.58	20.64	511.60	[29]
Iraq, Qayyarah	30.58	19.98	292.32	Present study

3.2 Basic Statistics

The statistical analysis in this paper was performed using SPSS version 23.0 for Windows, a statistics software program.The basic statistical variables for radionuclides (^{232}Th, ^{226}Ra, and ^{40}K) are measured and presented in Table 3, which are mean, median, kurtosis, deviation, and standard deviation. Kurtosis is a measure of the peakedness of a real-valued random variable's probability distribution. It describes a distribution's relative peakedness or flatness in comparison to the normal distribution. Positive Kurtosis denotes a distribution that is substantially peaked. A flat distribution is indicated by a negative kurtosis. Higher kurtosis indicates that infrequent extreme deviations account for more variation than frequent small deviations [16].

Table 3. Statistical variables of the investigated soil samples.

Variables	Statistical variables		
	^{226}Ra	^{232}Th	^{40}K
Mean	30.58	19.98	292.32
Median	31.75	19.13	270
Std. Deviation	10.15	5.92	135.08
Variance	103.05	35.15	18248.92
Skewness	0.39	0.56	0.89
Kurtosis	-0.04	-0.67	0.46
Minimum	14.3	12.6	131.9
Maximum	53.7	32.5	597.3
Range	39.4	19.9	465.4
Mean	30.58	19.98	295.81
Median	31.75	19.13	270
Std. Deviation	10.15	5.92	135.08
Variance	103.05	35.15	18248.92
Skewness	0.39	0.56	0.89
Kurtosis	-0.04	-0.67	0.46
Minimum	14.3	12.6	131.9
Maximum	53.7	32.5	597.3
Range	39.4	19.9	465.4

3.3 Box plot

A box plot, also referred to as a box-and-whisker diagram, is a graphical tool used to visualize the distribution of a data set. It offers a concise summary of several statistical measures, including the median, the first and third quartiles, and any outliers present in the data. One kind of statistical graphic that offers a visual representation of a dataset's distribution is a box plot The ends of the boxes indicate the minimum and maximum values of the dataset. The line inside the box represents the median (Q2). It divides the data into two halves, with 50% of the data falling below and 50% above this value. The bottom of the box represents the first quartile (Q1). This is the value below which 25% of the data falls. The top of the box represents the third quartile (Q3). This is the value below which 75% of the data falls. When comparing the distributions of several datasets, box plots come in handy since they make it simple to spot variations in skewness, dispersion, and central tendency. Figure 6 shows a box plot showing how specific activities for ^{226}Ra, ^{232}Th, and ^{40}K in (Bq/kg) spread out. The median is around the center of the ^{226}Ra and ^{40}K box, indicating that the data set's distribution is symmetrical and regularly distributed. The ^{232}Th median is closer to the box's bottom, and the distribution is skewed [16].

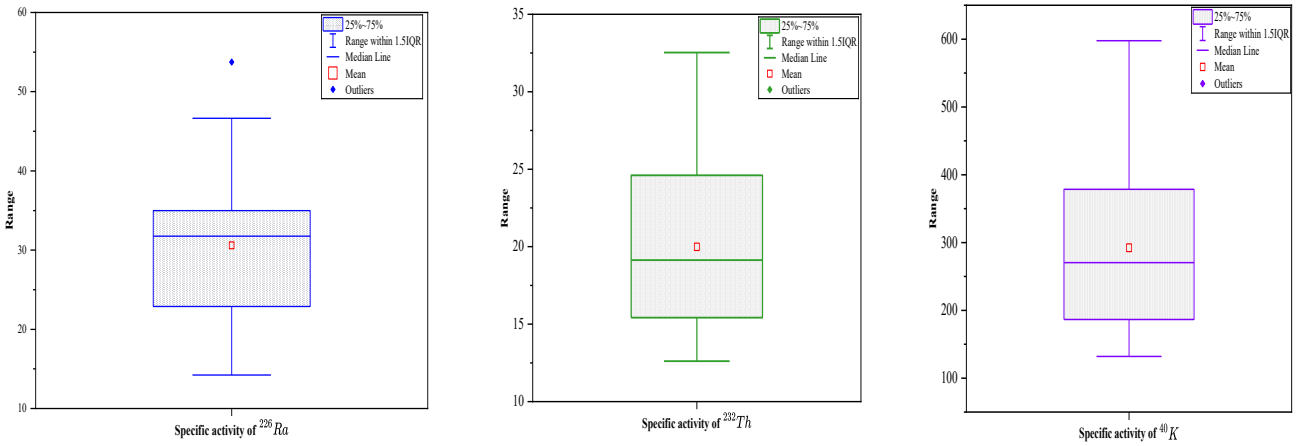

Figure 6. Box plot of ^{226}Ra, ^{232}Th and ^{40}K of the investigated soil samples.

3.4 Frequency distribution of radionuclides and Q-Q plot

The patterns and trends of radioactive decay can be understood by examining the frequency distribution of radionuclides in environmental samples. A graphical tool called a Q-Q (Quantile-Quantile) plot is used to determine if a dataset conforms to a specific probability distribution, like the normal distribution. Diffequencies from the predicted pattern can be used to identify non-normal behavior or outliers in the radionuclide measurements by displaying the quantiles of the observed data against the quantiles of the theoretical distribution. Figure 7 shows the frequency distribution and quantitative (Q-Q) plots for a given activity of ^{226}Ra, ^{232}Th and ^{40}K, as well as histograms. The distribution of the ^{40}K and ^{226}Ra radionuclides is normal (bell-shaped distribution). However, ^{232}Th has a multimodal logarithmic normal distribution. The complexity of radionuclides in soil samples is illustrated by the multimedia properties. Figure 7 shows a Q–Q plot where all points are approximately parallel to the 45° reference line and the distributions are assumed to be normal [17]. Based on the measured specific activities of the detected radionuclides in the soil samples, the radiological risk indices including the radium equivalent activity, the absorbed gamma dose rate, the annual effective dose, the external hazard index, the external gamma activity, the gamma representative level index, the excess lifetime cancer risk, and the annual gonadal dose equivalent were calculated using equations (3-10). The results are presented in Table 2. The values of radium equivalent, radiation absorbed dose, and annual effective dose (both indoor and outdoor) were calculated from soil samples and are presented in Table 4. The calculated radium equivalent (Ra_{eq}) ranged from 53.39 to 136.16 Bq/kg, with an average of 81.97 Bq/kg. The absorbed dose (D_R) ranged from 25.03 to 65.12 nGy/h, with an average of 38.55 nGy/h. The annual effective dose values were between 122.81 to 319.46 µSv/y for indoor, and 30.7 to 79.86 µSv/y for outdoor. All of the calculated radium equivalent and radiation absorbed dose values were less than the world safety limit value. The calculated H_{ex} index values ranged from 0.14 to 0.37, with an averge value of 0.22. The H_{in} index values were found to be between 0.18 and 0.51, with an averge of 0.30. The levels of H_{ex} and H_{in} were lower than the global average limit of 1 or less [14], which means that the radiation exposure is insignificant. The gamma index (I_γ) was calculated using the specific activities of ^{226}Ra, ^{232}Th, and ^{40}K for the sampled locations, as shown in Table 4. The gamma index values ranged from 0.39 to 1.01, with a mean value of 0.60. This mean gamma index is lower than the world average gamma index of 1 [14]. Additionally, all of the annual effective dose values measured in the soil samples were also below the world safety limit. The ELCR values ranged from 107.46 to 279.52, with an arithmetic mean value of 165.48. The worldwide average ELCR is 290 [14]. The arithmetic mean of the ELCR values in the data set is lower than the world's average ELCR. The calculated values for the annual gonadal dose equivalent (AGDE) ranged from 175.8 µSv/year to 460.08 µSv/year, with an average of 271.05 µSv/year. This average AGDE value is lower than the worldwide average of 300 µSv/y [14, 18], indicating that the AGDE values observed in this study are within the worldwide range, except for the sites (Qa3, Qa11, Qa15, Qa18, Qa21). This suggests that the AGDE values do not indicate any significant radiological risks. Therefore, there is no clear health hazard to people.

Table 4. Radiological hazard indices of soil samples near oil wells from the studied areas.

Sample ID	Radiological hazard indices								
	Ra_{eq} (Bq/kg)	D_R (nGy/h)	$AEDE_{in}$ (μSv/y)	$AEDE_{out}$ (μSv/y)	ELCR	H_{ex}	H_{in}	I_γ	AGDE (μSv/y)
Qa1	73.93	34.23	167.94	41.99	146.95	0.20	0.27	0.54	239.54
Qa2	75.98	36.78	180.44	45.11	157.88	0.21	0.28	0.57	261.50
Qa3	107.83	50.51	247.79	61.95	216.82	0.29	0.38	0.79	355.92
Qa4	91.85	42.49	208.43	52.11	182.38	0.25	0.35	0.66	295.70
Qa5	60.68	27.96	137.17	34.29	120.02	0.16	0.22	0.44	195.51
Qa6	53.54	25.52	125.21	31.30	109.56	0.14	0.19	0.40	181.38
Qa7	69.33	32.32	158.55	39.64	138.73	0.19	0.25	0.51	227.11
Qa8	53.97	25.84	126.78	31.70	110.94	0.15	0.18	0.41	184.20
Qa9	64.80	30.86	151.39	37.85	132.46	0.18	0.23	0.48	218.87
Qa10	53.39	25.03	122.81	30.70	107.46	0.14	0.20	0.39	175.80
Qa11	102.33	48.54	238.14	59.53	208.37	0.28	0.40	0.75	340.57
Qa12	91.96	41.47	203.46	50.86	178.03	0.25	0.34	0.65	286.72
Qa13	75.77	34.99	171.67	42.92	150.21	0.20	0.29	0.54	243.45
Qa14	77.51	37.33	183.11	45.78	160.22	0.21	0.28	0.58	265.09
Qa15	87.31	41.82	205.13	51.28	179.49	0.24	0.33	0.65	295.60
Qa16	136.16	65.12	319.46	79.86	279.52	0.37	0.51	1.01	460.08
Qa17	78.99	35.83	175.77	43.94	153.80	0.21	0.30	0.56	247.92
Qa18	94.90	46.62	228.69	57.17	200.10	0.26	0.33	0.73	334.97
Qa19	85.30	38.84	190.55	47.64	166.73	0.23	0.34	0.60	268.02
Qa20	84.34	40.28	197.62	49.40	172.92	0.23	0.32	0.63	284.59
Qa21	101.55	47.20	231.52	57.88	202.58	0.27	0.39	0.73	329.56
Max	136.16	65.12	319.46	79.86	279.52	0.37	0.51	1.01	460.08
Min	53.39	25.03	122.81	30.70	107.46	0.14	0.18	0.39	175.8
Average	81.97	38.55	189.13	47.28	165.48	0.22	0.30	0.60	271.05

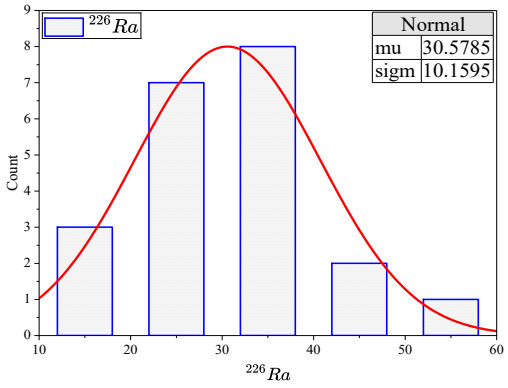

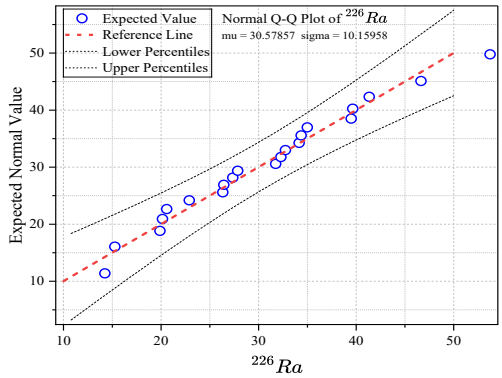

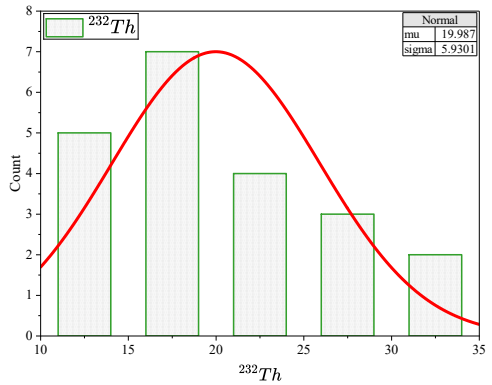

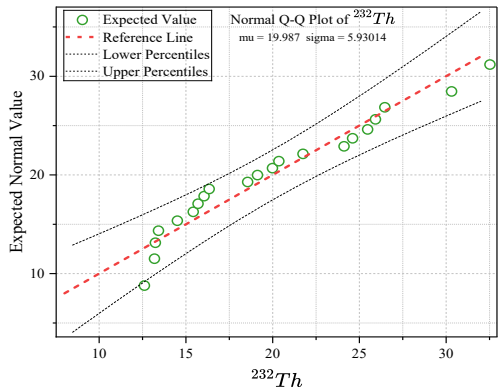

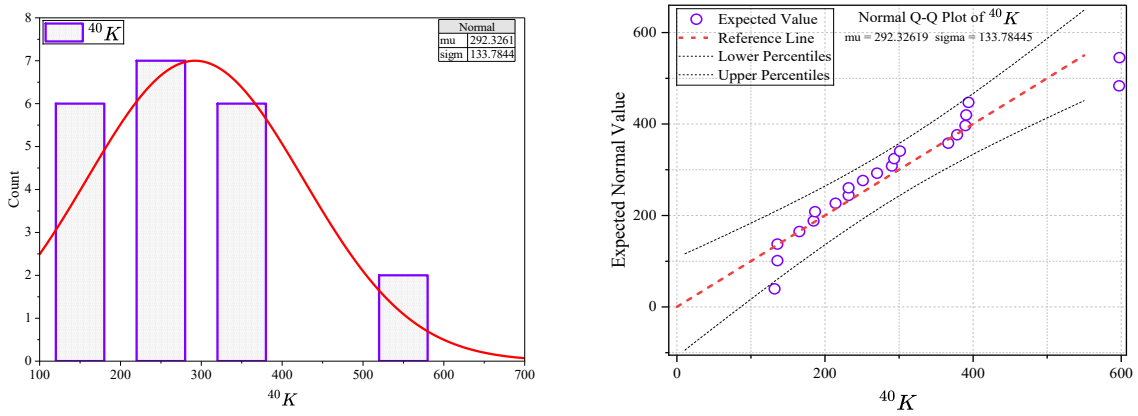

Figure 7. Frequency distribution and Quantile-quantile (Q-Q) plots of the activity concentrations for ^{226}Ra, ^{232}Th and ^{40}K of the investigated soil samples.

3.5 Pearson correlation coefficients

Pearson correlation coefficientis a statistical measure that quantifies the linear relationship between two variables. It ranges from -1 to 1, where 1 indicates a perfect positive linear relationship, -1 indicates a perfect negative linear relationship, and 0 indicates no linear relationship [10]. The correlation analysis was carried out as binary statistics in order to determine the interrelationship and the strength of the correlation between the pairs of variables as in Table 5. It was found that (^{232}Th) has a moderate direct correlation with (^{226}Ra) with a value of (0.596) and with (^{40}K) a weak inverse correlation with a value of (-0.213), and a direct and significant correlation between risk indicators with (^{226}Ra, ^{232}Th, and ^{40}K). The linear links between the variables under study are illuminated by these correlation coefficients. Perfect, strong correlations show a highly significant and strong link, whereas weak correlations point to a low degree of association. Researchers can gain insight into the interdependencies and possible links among the variables by examining the observed correlations between them.

Table 5. Pearson correlation matrix between radionuclides and their respective radiological hazard parameters.

Variables	Pearson correlation coefficients									
	^{226}Ra	^{232}Th	^{40}K	Ra_{eq}	D_R	H_{ex}	I_γ	H_{in}	$AEDE_{out}$	ELCR
^{226}Ra	1	0. 596	0.316							
^{232}Th	0.596	1	-0.213							
^{40}K	0.316	-0.213	1							
Ra_{eq}	0.337	-0.183	1	1						
D	0.339	-0.180	0.999	1	1					
H_{ex}	0.337	0.183	1	1	1	1				
I_γ	0.336	-0.185	1	1	1	1	1			
H_{in}	0.357	-0.153	0.998	1	1	1	0.999	1		
$AEDE_{out}$	0.339	-0.180	0.999	1	1	1	1	1	1	
ELCR	0.339	-0.180	0.999	1	1	1	1	1	1	1

3.6 Principal component analysis

Principal Component Analysis (PCA) is a widely-used dimensionality reduction method in data analysis and machine learning. The goal of PCA is to find a lower-dimensional representation of the original data while retaining as much of the original information as possible. The fundamental principle behind PCA is to identify the directions (principal components) in the original high-dimensional space that account for the greatest variance in the data. These principal components are mutually orthogonal and are ranked by the amount of variance they explain. Principal components analysis (PCA) was applied to identify variables by applying rotation (Varimax), where the factor was analyzed into two factors with a distinct value that explains (97.84168%) of the total variance. The rotation area for the first component (1) and the second component (2) is given in Table 6. The first component represents (87.26426%) of the total variance, and is mainly characterized by a high positive loading in concentrations (^{226}Ra, ^{40}K) as well as radiation risk indicators. The second component (10.57742%) of the total variance mainly represents the positive loading for (^{232}Th). The graphical representation of the 1

and 2 components is shown in Figure 8. These results show that the first component that explains most of the total variance is mainly associated with the concentrations of ^{226}Ra, ^{40}K isotopes, while the second component is mainly associated with ^{232}Th activity.

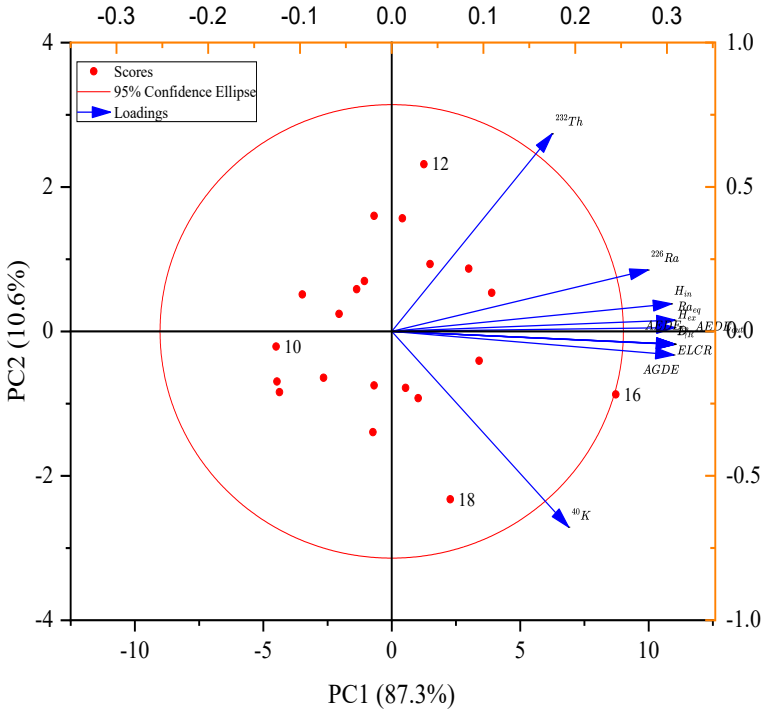

Figure 8. Components 1 and 2 represented graphically

3.7 Cluster Analysis

Cluster Analysis (CA) is a technique for identifying and classifying groups with comparable characteristics in new data. Each observation in a cluster is the most similar to the other observations in the cluster. The maximum distance between any two variables is used to calculated the distance between clusters. In sample measurements, the zero distance implies that the clusters are identical, whereas cluster areas are as dissimilar as the least similar region implying that they are 0% similar in size. Axes were used in the cluster analysis to discover similarities between natural radio-isotopes and radiological parameters in soils. The average linkage approach was used in CA, coupled with the correlation coefficient distance, and the resulting dendrogram was exhibited in Figure 9 and the cluster membership was shown in Table 6. the variables are categorized in three stages. All ten parameters are sorted into four statistically significant clusters in this dendrogram. Cluster I comprised of a constant of ^{226}Ra, cluster II of ^{232}Th, cluster III of ^{40}K, and cluster IIII of other radiological parameter distributions that appeared in the same cluster in the first stage. The second stage included three clusters, with the fourth cluster's variables blended with the first clusters. The variables from the third cluster were combined with those from the second cluster in the third step.

Table 6. Cluster Membership, and rotated factors of the variables

Variables	Cluster Membership			Rotated factors	
	4 Clusters	3 Clusters	2 Clusters	1 Component	2 Component
^{226}Ra	1	1	1	0.27942	0.21277
^{232}Th	3	3	2	0.17507	0.68423
^{40}K	2	2	1	0.19296	-0.67763
Ra_{eq}	4	1	2	0.30867	0.03919
D_R	4	1	2	0.30855	-0.0444
$AEDE_{in}$	4	1	2	0.30855	-0.04436
$AEDE_{out}$	4	1	2	0.30855	-0.04433
ELCR	4	1	2	0.30855	-0.04433
H_{ex}	4	1	2	0.3086	0.0128
H_{in}	4	1	2	0.30505	0.09564
I_γ	4	1	2	0.30835	-0.04532

AGDE	4	1	2	0.30753	-0.08127

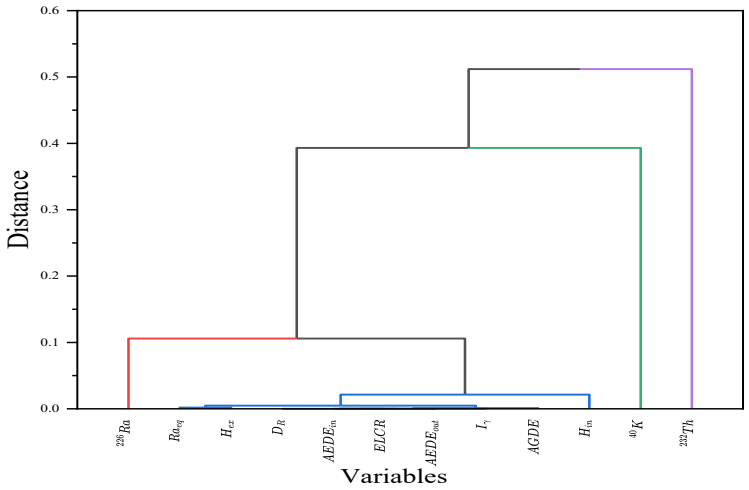

Figure 9. Dendrogram shows the clustering of radiological parameters.

4. CONCLUSION

The specific activites of the investigated soil samples ranged from 14.24±0.66 to 53.73±1.29 Bq/kg for ^{226}Ra, 12.61±0.92 to 32.53±1.41 Bq/kg for ^{223}Th, and 131.90±7.12 to 597.69±15.15 Bq/kg for ^{40}K. The measured specific activity of ^{40}K was higher than that of both ^{226}Ra and ^{223}Th, indicating that ^{40}K is a more abundant radioactive element than the other elements in the studied soils. The activity concentrations observed in many of the investigated soil samples exceeded the recommended world values. This can be attributed to the fact that the samples were collected from areas surrounding an oil refinery and oil wells. The average values of the radiological hazard parameters obtained, such as radium equivalent, absorbed dose rate, annual effective dose equivalent, gamma representative index, annual gonadal dose equivalent, external hazard index, and internal hazard index, were within the recommended world values. The study concluded that no radiological impacts were imposed on the workers and residents living near the study area. The data obtained from this study provides baseline information that can be helpful in setting national screening levels for exposure to Naturally Occurring Radioactive Materials (NORM) in different activities. This baseline data can also aid in developing national control regulations for industries dealing with NORM.

ACKNOWLEDGEMENTS

The authors express their thanks and appreciation to the Department of Physics in the Faculty of Science, University of Mosul for its continuous support.

REFERENCES

[1] Ramadhan, H. H., & Kim, J. (2021). Radiological Risk Assessment of Vehicle Transport Accidents Associated with Consumer Products Containing Naturally Occurring Radioactive Materials. *Applied Sciences, 11*(18), 8719.

[2] Alam, I., Rehman, J. U., Ahmad, N., Nazir, A., Hameed, A., & Hussain, A. (2020). An overview on the concentration of radioactive elements and physiochemical analysis of soil and water in Iraq. *Reviews on environmental health, 35*(2), 147-155.

[3] Guidebook, A. (1989). Measurement of Radionuclides in Food and the Environment. *Vienna: International Atomic Energy Agency.*

[4] Faweya, E. B., Alabi, F. O., & Adewumi, T. (2014). Determination of radioactivity level and hazard assessment of unconsolidated sand and shale soil samples from petroleum oil field at Oredo, Benin, Niger Delta-Nigeria. *Archives of Applied Science Research, 6*(2), 76-81.

[5] Najam, L. A., & Marie, Z. M. (2022). Evaluation of natural radioactivity and radiological hazard indicators in soil samples from the environment of Al-Kasik oil refinery in Nineveh Governorate, Iraq. *Arab Journal of Nuclear Sciences and Applications*, *55*(4), 57-66.

[6] Sayyed, M. I., Maria, Z. M., Hussein, Z. A., Najam, L. A., Namq, B. F., Wais, T. Y., ... & Mansour, H. (2024). Radiological hazard assessment of soil from Kasik oil refinery, Nineveh, Iraq. *Nuclear Engineering and Technology.*

[7] Najam, L. A., Al-Dbag, S. T., Wais, T. Y., & Mansour, H. (2022). Radiogenic heat production from natural

radionuclides in sediments of the Tigris river in Mosul City, Iraq. *International Journal of Nuclear Energy Science and Technology, 15*(3-4), 302-316.

[8] Wais, T. Y., & Najam, L. A. (2021, September). Activity Concentration of Natural Radionuclides in Sediment of Tigris River in the City of Mosul, Iraq. In *Journal of Physics: Conference Series* (Vol. 1999, No. 1, p. 012064). IOP Publishing

[9] Najam, L. A., Ahmed, I., Alkhayat, R. B., & Wais, T. Y. (2022). Transfer factors of 226Ra, 232Th and 40K from fertilised soil to different types of field crops in Tikrit city, Iraq. *International Journal of Nuclear Energy Science and Technology, 16*(1), 31-43.

[10] Wais, T. Y., Ali, F. N. M., Najam, L. A., Mansour, H., & Mostafa, M. Y. A. (2023). Assessment of natural radioactivity and radiological hazards of soil collected from Rabia town in Nineveh Governorate (North Iraq). *Physica Scripta, 98*(6), 065304.

[11] Alkhayat, R. B., Najam, L. A., Wais, T. Y., & Mansour, H. (2023). Evaluation of radiological risk of uranium in well water in Nineveh Governorate, northern Iraq. *International Journal of Nuclear Energy Science and Technology*, *16*(3), 157-168.

[12] Siraz, M. M., Dewan, M. J., Chowdhury, M. I., Al Mahmud, J., Alam, M. S., Rashid, M. B., ... & Yeasmin, S. (2023). Radioactivity in soil and coal samples collected from the vicinity of the coal-fired thermal power plant and evaluation of the associated hazard parameters. *International Journal of Environmental Analytical Chemistry*, 1-18.

[13] Beretka, J., & Mathew, P. J. (1985). Natural radioactivity of Australian building materials, industrial wastes and by-products. *Health physics, 48*(1), 87-95.

[14] United Nations Scientific Committee on the Effects of Atomic Radiation. (2000). *Sources and Effects of Ionizing Radiation, United Nations Scientific Committee on the Effects of Atomic Radiation (UNSCEAR) 2000 Report, Volume I: Report to the General Assembly, with Scientific Annexes-Sources*. United Nations.

[15] Najam, L. A., & Wais, T. Y. (2022). Radiological hazard assessment of radionuclides in sediment samples of Tigris river in Mosul city, Iraq. *Arab Journal of Nuclear Sciences and Applications, 55*(1), 45-52.

[16] Harikrishnan, N., Ravisankar, R., Chandrasekaran, A., Gandhi, M. S., Vijayagopal, P., & Mehra, R. (2018). Assessment of gamma radiation and associated radiation hazards in coastal sediments of south east coast of Tamilnadu, India with statistical approach. *Ecotoxicology and Environmental safety, 162*, 521-528.

[17] SureshGandhi, M., Ravisankar, R., Rajalakshmi, A., Sivakumar, S., Chandrasekaran, A., & Anand, D. P. (2014). Measurements of natural gamma radiation in beach sediments of north east coast of Tamilnadu, India by gamma ray spectrometry with multivariate statistical approach. *Journal of Radiation Research and Applied Sciences, 7*(1), 7-17.

[18] Nations, U. (1993). Sources and effects of ionizing radiation. *UNSCEAR Report*.

[19] Durusoy, A., & Yildirim, M. (2017). Determination of radioactivity concentrations in soil samples and dose assessment for Rize Province, Turkey. *Journal of Radiation Research and Applied Sciences*, *10*(4), 348-352.

[20] Hussein, Z. A. (2019). Assessment of natural radioactivity levels and radiation hazards for soil samples used in Erbil governorate, Iraqi Kurdistan. *ARO-The Scientific Journal of Koya University*, *7*(1), 34-39.

[21] Sethy, N. K., Jha, V. N., Sutar, A. K., Rath, P., Sahoo, S. K., Ravi, P. M., & Tripathi, R. M. (2014). Assessment of naturally occurring radioactive materials in the surface soil of uranium mining area of Jharkhand, India. *Journal of Geochemical Exploration*, *142*, 29-35.

[22] Jibiri, N. N., & Amakom, C. M. (2011). Radiological assessment of radionuclide contents in soil waste streams from an oil production well of a petroleum development company in Warri, Niger Delta, Nigeria. *Indoor and Built Environment*, *20*(2), 246-252.

[23] Jibiri, N. N., & Amakom, C. M. (2011). Radiological assessment of radionuclide contents in soil waste streams from an oil production well of a petroleum development company in Warri, Niger Delta, Nigeria. *Indoor and Built Environment*, *20*(2), 246-252.

[24] Khan, H. M., Ismail, M., Zia, M. A., & Khan, K. (2012). Measurement of radionuclides and absorbed dose rates in soil samples of Peshawar, Pakistan, using gamma ray spectrometry. *Isotopes in environmental and health studies*, *48*(2), 295-301.

[25] Suresh, S., Rangaswamy, D. R., Srinivasa, E., & Sannappa, J. (2020). Measurement of radon concentration in drinking water and natural radioactivity in soil and their radiological hazards. *Journal of radiation research and applied sciences*, *13*(1), 12-26.

[26] Malik, F., Matiullah, Akram, M., & Rajput, M. U. (2011). Measurement of natural radioactivity in sand samples collected along the bank of rivers Indus and Kabul in northern Pakistan. *Radiation Protection Dosimetry*, *143*(1), 97-105.

[27] Alshahri, F., & El-Taher, A. (2019). Investigation of Natural Radioactivity Levels and Evaluation of Radiation Hazards in Residential-Area Soil Near a Ras Tanura efinery, Saudi Arbia. *Polish Journal of Environmental Studies*, *28*(1).

[28] Ahmed, M. M., Das, S. K., Haydar, M. A., Bhuiyan, M. M. H., Ali, M. I., & Paul, D. (2014). Study of natural radioactivity and radiological hazard of sand, sediment, and soil samples from Inani Beach, Cox's Bazar, Bangladesh. *Journal of Nuclear and Particle Physics*, *4*(2), 69-78.

[29] Albıdhanı, H., Gunoglu, K., & Akkurt, İ. (2019). Natural radiation measurement in some soil samples from Basra oil field, IRAQ State. *International Journal of Computational and Experimental Science and Engineering*, *5*(1), 48-51.